nature biotechnology

Virus stamping for targeted single-cell infection *in vitro* and *in vivo*

Rajib Schubert[1,7], Stuart Trenholm[2,6,7], Kamill Balint[2,3,7], Georg Kosche[2], Cameron S Cowan[2], Manuel A Mohr[1], Martin Munz[2], David Martinez-Martin[1], Gotthold Fläschner[1], Richard Newton[1], Jacek Krol[2], Brigitte Gross Scherf[2], Keisuke Yonehara[2,6], Adrian Wertz[2], Aaron Ponti[1], Alexander Ghanem[4], Daniel Hillier[2], Karl-Klaus Conzelmann[4], Daniel J Müller[1] & Botond Roska[2,5]

Genetic engineering by viral infection of single cells is useful to study complex systems such as the brain. However, available methods for infecting single cells have drawbacks that limit their applications. Here we describe 'virus stamping', in which viruses are reversibly bound to a delivery vehicle—a functionalized glass pipette tip or magnetic nanoparticles in a pipette—that is brought into physical contact with the target cell on a surface or in tissue, using mechanical or magnetic forces. Different single cells in the same tissue can be infected with different viruses and an individual cell can be simultaneously infected with different viruses. We use rabies, lenti, herpes simplex, and adeno-associated viruses to drive expression of fluorescent markers or a calcium indicator in target cells in cell culture, mouse retina, human brain organoid, and the brains of live mice. Virus stamping provides a versatile solution for targeted single-cell infection of diverse cell types, both *in vitro* and *in vivo*.

The ability to genetically engineer single cells, including via virus infection, facilitates analysis of the role of specific cell types in complex tissues[1–3]. In brain research, infection of single cells with one or more viruses has several applications including monosynaptic circuit tracing[4–6], and studying the formation of circuits[7], the roles of specific genes in particular cell types[8–10], and the development of single neuronal progenitors[11,12] in brain tissues or in brain organoids[13–15].

Current methods for infecting single cells have opened exciting possibilities to genetically manipulate and understand the physiology of single cells[6,16]. However, these methods either show limited applicability in tissues and *in vivo* or are technically complex to perform. Atomic force microscopy was used to infect cells with vaccinia viruses in combination with microcantilevers[17,18], but is limited to cell culture; push-pull microfluidic virus delivery was used for rabies virus infection[19], but is limited for use *in vitro* on tissue surfaces; single-cell electroporation or whole-cell patch clamp to deliver a plasmid to express a virus receptor in combination with bulk rabies virus loading is the state of the art *in vivo* approach[4–6], however, its efficacy is low and it is technically difficult to perform.

We aimed to develop a simple and versatile system for single-cell infection that fulfills the following criteria: (i) it can be used with a variety of viruses and cell types; (ii) it allows for co-infection of individual cells with different types of viruses; (iii) it can be used *in vitro* and *in vivo*. With 'virus stamping', viruses are delivered to target cells by physical contact with a virus stamper. The technical details for the virus stamper vary based on whether the application is targeting a cell on a surface or within a tissue.

For stamping cells on surfaces we developed an unshielded virus stamper in which a virus bound to a blunt glass pipette tip is brought into physical contact with the cell body of a single cell. For stamping cells within tissues we developed a shielded virus stamper in which a virus is bound to magnetic nanoparticles inside a glass pipette. The tip of the glass pipette is placed adjacent to the cell body of a single cell and the nanoparticles are brought into contact with the cell by magnetic attraction.

We validated virus stamping by infecting single cells with either vesicular stomatitis virus envelope glycoprotein (VSVG)-coated lenti[20] or VSVG-coated G-deleted rabies[21,22] viruses in cell culture, in mouse brain slice, in mouse retina, in human brain organoid, as well as *in vivo* in mouse cortex. We demonstrate the versatility of virus stamping by infecting neighboring cells with different viruses, by infecting a single cell with multiple types of viruses, by performing monosynaptically restricted trans-synaptic circuit tracing with rabies virus[4–6], by performing *in vivo* two-photon calcium imaging of virus-stamped cells, and by using other viruses including herpes simplex and adeno-associated viruses (AAVs).

RESULTS

The design of viruses for virus stamping

The first step of virus stamping is the binding of viruses to a mechanical carrier, such as a glass pipette, using chemical linkers (**Fig. 1a**). A problem related to binding different types of viruses to the same mechanical carrier is the variable surface properties of viruses, which are largely determined by glycoproteins. To make virus stamping versatile, one

[1]Department of Biosystems Science and Engineering, ETH Zurich, Basel, Switzerland. [2]Neural Circuit Laboratories, Friedrich Miescher Institute for Biomedical Research, Basel, Switzerland. [3]University of Basel, Basel, Switzerland. [4]Max von Pettenkofer-Institute & Gene Center, Faculty of Medicine, Ludwig-Maximilians-University Munich, Munich, Germany. [5]Department of Ophthalmology, University of Basel, Basel, Switzerland. [6]Present addresses: Montreal Neurological Institute, McGill University, Montreal, Quebec, Canada (S.T.) and The Danish Research Institute of Translational Neuroscience, Aarhus University, Aarhus, Denmark (K.Y.). [7]These authors contributed equally to this work. Correspondence should be addressed to D.J.M. (daniel.mueller@bsse.ethz.ch) or B.R. (botond.roska@fmi.ch).

Received 29 August; accepted 13 November; published online 18 December 2017; doi:10.1038/nbt.4034

would need either different chemical linkers, each of which specifically binds a certain type of virus, or a single chemical linker that more flexibly attaches to different viruses. We focused on the latter because it simplifies the combinatorial use of different viruses for stamping. Many viruses that are used to transduce cells, including lenti, rabies, and herpes simplex viruses, are enveloped[23]. The viral envelope is composed of lipid membrane that incorporates viral glycoproteins, and this determines the cell types and the area of the target cell where the virus can enter (e.g., cell body vs. axon terminal[21]). Viral glycoproteins can be exchanged across different enveloped viruses, a process called pseudotyping[21]. We chose VSVG[20,24] as the virus coat for stamping because it allows efficient viral entry at the cell body of most cell types, including adult neurons[21,22]. We initially focused on VSVG-coated lenti[20] and VSVG-coated G-deleted rabies[21,22] viruses.

Virus stamping for targeting cells located on a surface

We bound viruses to the flame-blunted tip of a glass patch pipette using a chemical 'glass linker' and brought the pipette tip into physical contact with the cell body of a single cell, enabling virus binding and entry to the target cell (**Fig. 1a**,**b** and **Supplementary Fig. 1a–d**). We used two avenues to find a suitable glass linker to bind VSVG-coated viruses to the tip of the glass pipette. The first was based on the putative electrostatic binding of the glass linker to the negatively charged VSVG-coated viruses[25–27]. We functionalized glass pipettes with various cationic polymers including polybrene[28], polyethyleneimine[29], or N^1-(3-trimethoxysilylpropyl)diethylenetriamine[30] (AEEA). The second relied on specific binding of the glass linker to sugar residues in VSVG[31] and involved functionalizing glass pipettes with concanavalin-A, a lectin known to bind mannose residues with high affinity, which has previously been used to immobilize viruses[32]. To determine the efficacy of these approaches, we examined the density of viruses that bound to the pipette tips using scanning electron microscopy (**Fig. 1c–f**). We found AEEA to be the most effective glass linker (**Fig. 1c**). Next, we tested different buffer solutions to bind viruses to glass via AEEA, and found that NTE buffer[21] was more effective than PBS buffer[33] ($P < 0.01$, $n = 5$, Mann–Whitney U-test).

To test whether virus particles stayed bound to the pipette tip when placed in a liquid medium, we immersed and then removed virus-coated pipettes from medium containing cultured cells, brain slices, or retinae. We observed non-targeted infection in less than 20% of the cases ($n = 6/33$). However, by diluting the virus we eliminated non-targeted infection at a concentration that was still high enough to allow for targeted single-cell infection ($n = 8$; **Supplementary Fig. 1e**).

To test whether the virus particles preferentially bound to the cell, we bound viruses to a functionalized pipette tip and placed the pipette tip in physical contact with a cell body for 1 min (**Supplementary Fig. 1f**). We then examined the pipette tip with scanning electron microscopy (**Fig. 1g**). We found that virus particles were effectively removed from the pipette tip at the location that had been in contact with the cell body.

Targeted infection of single cells with virus stamping

Next, we stamped single cells in culture with viruses encoding fluorescent proteins and tested infection by fluorescence expression. We targeted individual baby hamster kidney (BHK) cells using VSVG-coated lenti viruses encoding *tdTomato*. Stamping a single cell resulted in bright tdTomato expression after 1 d in culture (**Supplementary Fig. 1g**; $n = 6$). Similar targeted single-cell infection was achieved using VSVG-coated G-deleted rabies viruses encoding either *tdTomato* or *GFP* in neuronal cell culture (**Fig. 1h**; $n = 4$), and *ex vivo* in mouse brain slices (**Fig. 1i**; $n = 4$) and retina (**Fig. 1j**; $n = 4$).

We then combined virus stamping with two-photon microscopy and genetic labeling to target infection to single, pre-labeled neurons. For cultured neurons, we first transfected cells with low concentrations of *GFP*-encoding plasmids, resulting in sparse GFP expression, before stamping a single GFP-positive cell with VSVG-coated G-deleted rabies viruses encoding *tdTomato* (**Supplementary Fig. 2a**,**b**). For the retina, we used a mouse line in which melanopsin-expressing ganglion cells, which represent a subset of the total retinal ganglion cell population, also expressed tdTomato[34], and stamped a single tdTomato-positive cell with VSVG-coated G-deleted rabies viruses encoding *GFP* (**Fig. 1k**; $n = 6$). In both neuronal culture and on the surface of retina, the targeted pre-labeled cell, and no other cells, expressed both tdTomato and GFP.

The versatility of virus stamping

To assess the versatility of virus stamping for combinatorial labeling, we first targeted two different neighboring neurons in the same cell culture dish with different viruses using two different virus stampers. This resulted in bright fluorescence, with different fluorophores, in each neuron (**Fig. 2a**,**b**; $n = 4$). Second, we targeted individual neurons with a pipette tip to which had been bound both VSVG-coated lenti viruses encoding *GFP* and VSVG-coated G-deleted rabies viruses encoding *tdTomato* (**Fig. 2c**). In cell culture ($n = 3$), brain slices ($n = 3$), and retina ($n = 4$), the targeted cells became co-infected with both viruses in this one-step process, resulting in cells that expressed both GFP and tdTomato (**Fig. 2d** and **Supplementary Fig. 2c–f**). Third, we performed simultaneous co-infection to trace the neuronal circuit of the target cell using single-cell-initiated monosynaptic tracing[4–6]. We bound VSVG-coated G-deleted rabies viruses encoding *GFP* and VSVG-coated lenti viruses encoding *rabies-G* to the same pipette tips (**Fig. 2e**) and stamped individual cells. If both *rabies-G*-encoding lenti virus and *GFP*-encoding G-deleted rabies virus infect the target cell, we expect rabies-G to complement the G-deleted rabies virus and allow it to spread to neurons that are synaptically connected to the target cell. These connected neurons will then express GFP but will be unable to pass rabies in a retrograde manner to other neurons, because rabies-G is present only in the stamped starter neuron.

In retina (**Fig. 2f–j**; $n = 4$) and brain slices (**Supplementary Fig. 2g**,**h**; $n = 4$), we found multiple GFP-labeled neurons in the vicinity of the target cell. To ensure that the multitude of cells labeled with GFP was due to a rabies jump from a single cell and not to non-targeted infection, we performed immunohistochemistry for rabies-G protein and found that it was restricted to a single GFP-positive neuron, which represents the target cell (**Supplementary Fig. 2h**). As an additional control, we performed a three-dimensional (3D) reconstruction of the labeled neurons traced from a single target retinal cell (**Fig. 2g–i**). We found that the processes of both the target cell and the other GFP-labeled neurons (amacrine cells) stratified in the same layer of the inner plexiform layer in the retina (i.e., where synapses between amacrine and ganglion cells reside). In addition, when we closely examined the dendrites of the starter cell, we found contact points (which we consider to be putative synapses) with each of the GFP-labeled neurons (**Fig. 2j**).

Although we optimized virus stamping to work with VSVG-coated enveloped viruses, we also tested virus stamping with enveloped viruses not pseudotyped with VSVG, as well as with non-enveloped viruses. First, we stamped individual cultured neurons with VSVG-coated G-deleted rabies viruses encoding *GFP* ($t = 0$ h). Two days later ($t = 48$ h) we stamped the previously stamped cells with herpes simplex viruses (HSVs; non-VSVG-coated) encoding *mCherry*. By $t = 52$ h we found that stamped cells expressed both GFP and mCherry

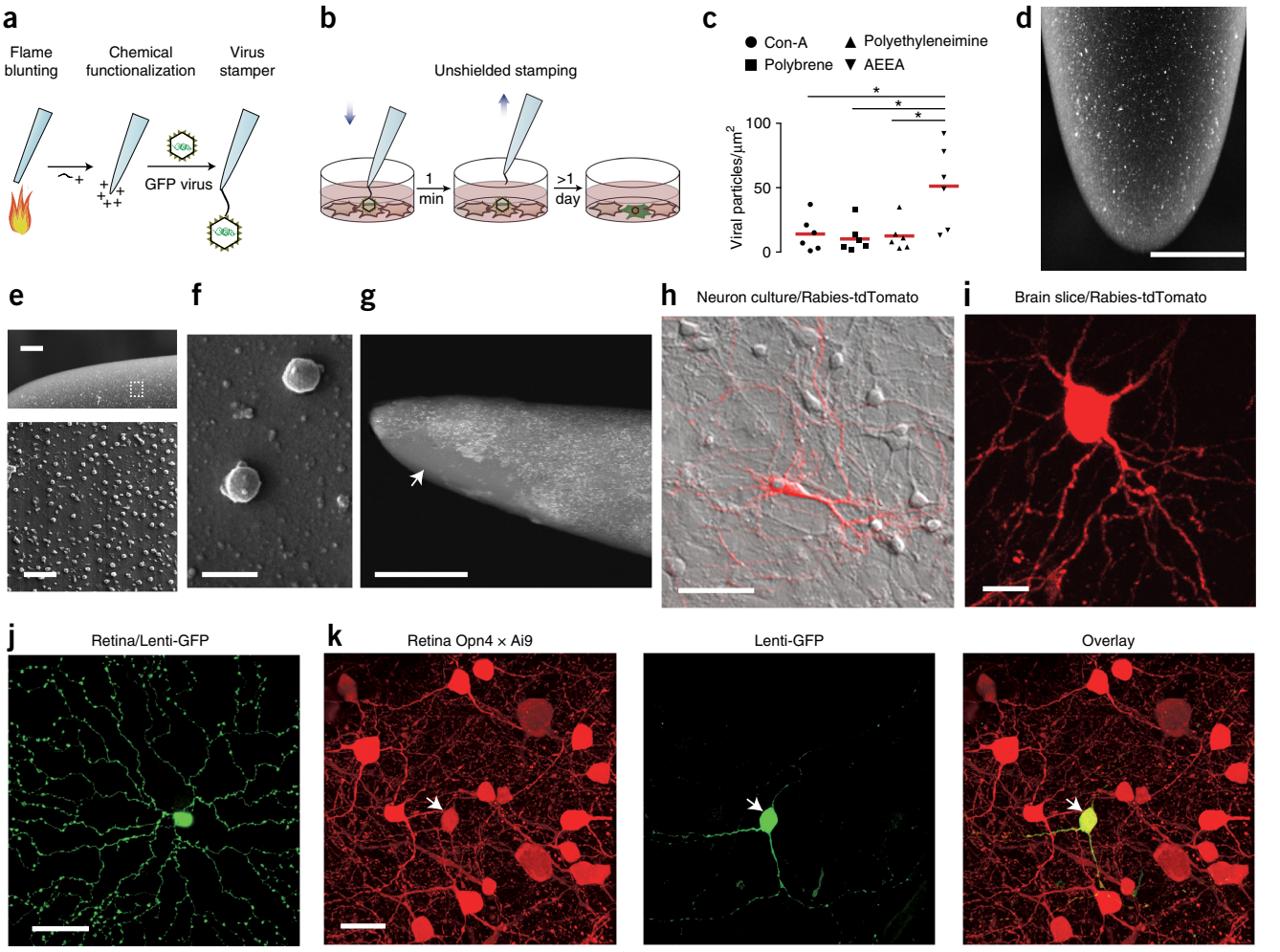

Figure 1 Single-cell virus stamping using an unshielded stamper. (**a**,**b**) Schematic representation of the key steps. After flame-blunting and cleaning a patch pipette, the tip of the pipette is functionalized with the glass linker, and the virus, here encoding *GFP*, is bound to the functionalized pipette (**a**). The virus-bound pipette is lowered into the solution and the cell body of a target cell is approached and mechanically touched (stamped) for 1 min. The pipette tip is then removed and the cells or tissue are cultured until virus infection drives expression of the fluorescent marker (**b**). (**c**) Number of virus particles bound to functionalized pipette tips. Flame-blunted patch pipettes were coated with concanavalin-A (Con-A), polybrene, polyethyleneimine, or AEEA and transferred to a solution containing VSVG-coated lenti viruses. The number of virus particles bound to pipettes were quantified by scanning electron microscopy (SEM) ($n = 6$ for each chemical, red bars represent the mean). (**d**) Low-magnification SEM of an AEEA-functionalized pipette tip carrying VSVG-coated lenti viruses. Scale bar, 5 µm. (**e**) Medium- (top) and high- (bottom) magnification SEM images of the functionalized pipette tip. Scale bars, 1 µm (top) and 400 nm (bottom). The dashed box in the top panel shows the field of view in the bottom panel. (**f**) Higher magnification of the image shown in the bottom panel of **e**. Scale bar, 100 nm. (**g**) SEM of a pipette tip after being used for virus stamping. The white arrow indicates a region with no bound virus, correlating to the part of the pipette tip that touched the cell during stamping. Scale bar, 5 µm. (**h**–**k**) Examples of single-cell infection of a neuron in culture (**h**), brain slice (**i**), and retina (**j**). Scale bars, 50 µm (**h**,**j**); 20 µm (**i**). The type of virus and the expressed protein is indicated above the panels. (**k**) Virus stamping of a single tdTomato-expressing ganglion cell in retina with VSVG-coated G-deleted rabies viruses encoding *GFP*. Left panel, tdTomato-expressing ganglion cells (in *Opn4*-Cre × Ai9 mice). Middle panel, GFP-expressing target cell. Right panel, overlay of tdTomato and GFP signals. Scale bar, 20 µm. White arrows show the target cell.

(**Supplementary Fig. 2i**–**k**; $n = 4$). Second, in a single stamping session we simultaneously stamped individual cultured cortical neurons with rabies-G-coated G-deleted rabies viruses (non-VSVG-coated) encoding *GFP* and HSVs (non-VSVG-coated) encoding *tdTomato*. We then imaged these cells at day 3, 5, and 7 after stamping, and found stable expression of both GFP and tdTomato across all days. The morphology of the stamped cells also appeared unchanged throughout this time (**Supplementary Fig. 3a**; $n = 3$). Third, we simultaneously stamped, in a single session, individual cultured cortical neurons with non-enveloped AAVs encoding *GCaMP6s* and AAVs encoding *mRuby* (**Supplementary Fig. 3b**). Two weeks after stamping, the stamped cells expressed both GCaMP6s and mRuby ($n = 6$).

Virus stamping for infecting single cells in tissue

The virus stamping approach presented so far is limited to infecting cells on the surface of a tissue because stamping deeper cells with virus-coated pipette tips would result in viruses being non-specifically rubbed off the pipette, causing off-target infection. We therefore developed a second approach, that we call shielded virus stamping, that is capable of infecting single cells deeper within tissue (**Fig. 3a**,**b**). Here, we bound viruses to the surface of magnetic nanoparticles and shielded them during tissue penetration by placing them inside a glass pipette, preventing non-specific infection. Once the pipette tip was adjacent to the target cell, the virus-bound magnetic nanoparticles were brought into contact with the membrane

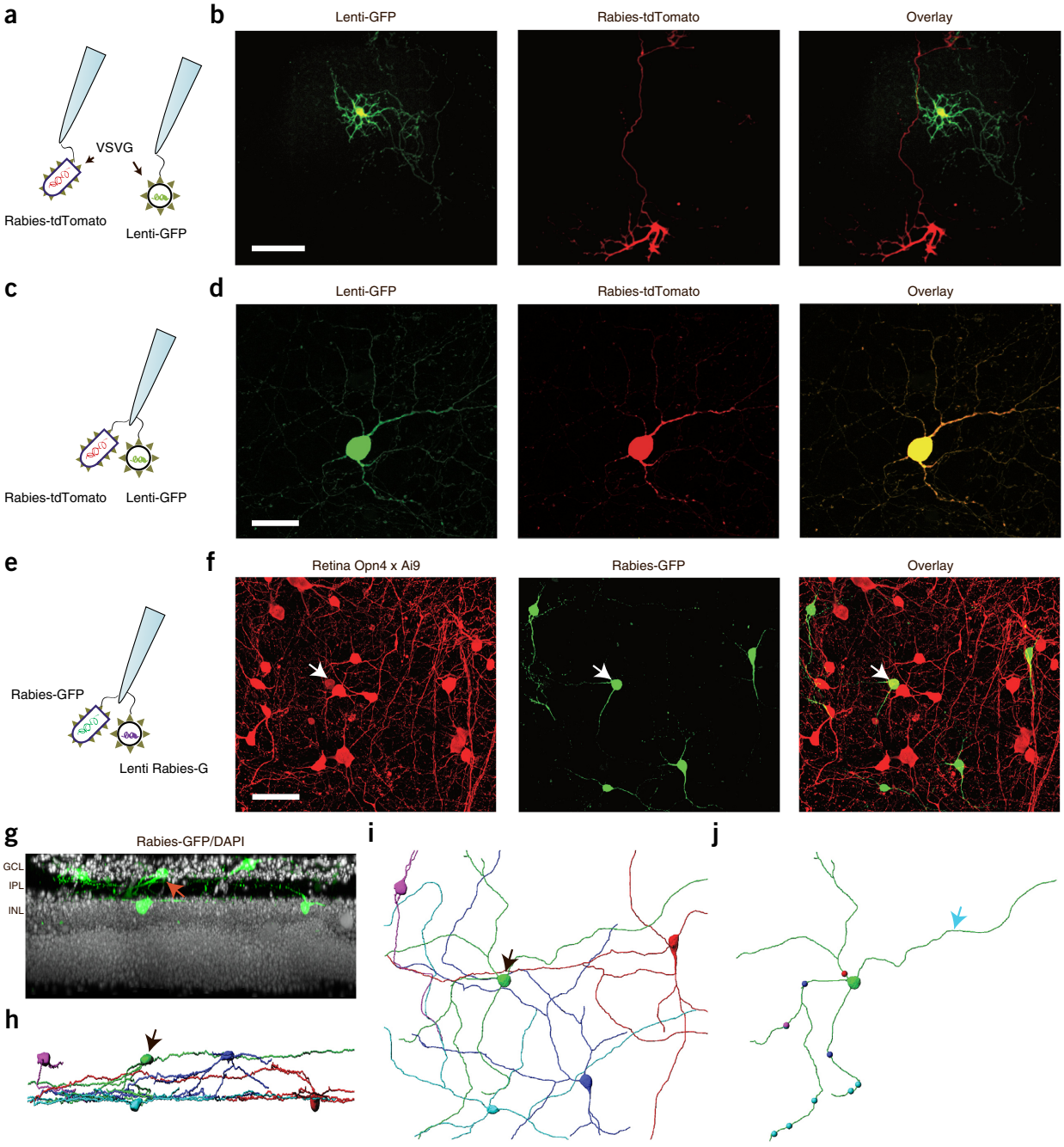

Figure 2 Versatility of virus stamping. (**a**,**b**) Infecting two neighboring cells with two different viruses. Two stampers were used, one with VSVG-coated G-deleted rabies viruses encoding *tdTomato* and the other with VSVG-coated lenti viruses encoding *GFP* bound to the surface (**a**). Example of two infected neighboring neurons in culture (**b**). Left panel, GFP-expressing cell. Middle panel, tdTomato-expressing cell. Right panel, overlay of GFP and tdTomato signals. Scale bar, 60 µm. (**c**,**d**) Co-infecting a single cell with two different viruses. A single stamper was used. It was bound with both VSVG-coated G-deleted rabies viruses encoding *tdTomato* and VSVG-coated lenti viruses encoding *GFP* (**c**). Example of a co-infected cell in retina (**d**). Left panel, GFP expression. Middle panel, tdTomato expression. Right panel, overlay of GFP and tdTomato signals. Scale bar, 30 µm. (**e**,**f**) Single-cell-initiated monosynaptic circuit tracing performed by infecting a single cell with two viruses. A single stamper was used. It was bound with both VSVG-coated G-deleted rabies viruses encoding *GFP* and VSVG-coated lenti viruses encoding the *rabies glycoprotein* (*Rabies-G*) (**e**). Example of a single-cell-initiated tracing of a neuronal circuit in retina (**f**). Left panel, a single tdTomato-expressing retinal ganglion cell (white arrow) was targeted in a retina in which a subset of ganglion cells express tdTomato (in *Opn4*-Cre × Ai9 mice). Middle image, virus stamping labeled the target ganglion cell with GFP (white arrow). In addition, several presynaptic amacrine cells were also labeled with GFP via trans-synaptic spread of the rabies virus from the target ganglion cell. Right image, overlay of tdTomato and GFP signals. Scale bar, 40 µm. (**g**) Side projection of the middle panel of **f** showing the location and stratification of all GFP-labeled cells. The red arrow indicates the starter cell. GCL, ganglion cell layer; IPL, to the inner plexiform layer; INL, the inner nuclear layer. To emphasize IPL boundaries, the retina was DAPI-labeled (white). (**h**) Computer reconstruction of GFP-labeled cells revealing that all neurons send processes into the same layer of the IPL. The starter cell is indicated with the black arrow. (**i**) Top view of the reconstruction. The starter cell is indicated with the black arrow. (**j**) The starter cell is color-coded with dots indicating contact points with presynaptic neurons labeled in **h** and **i**. The blue arrow indicates the axon of the starter cell (note that all presynaptic cells are lacking single axons, demonstrating that they are amacrine cells).

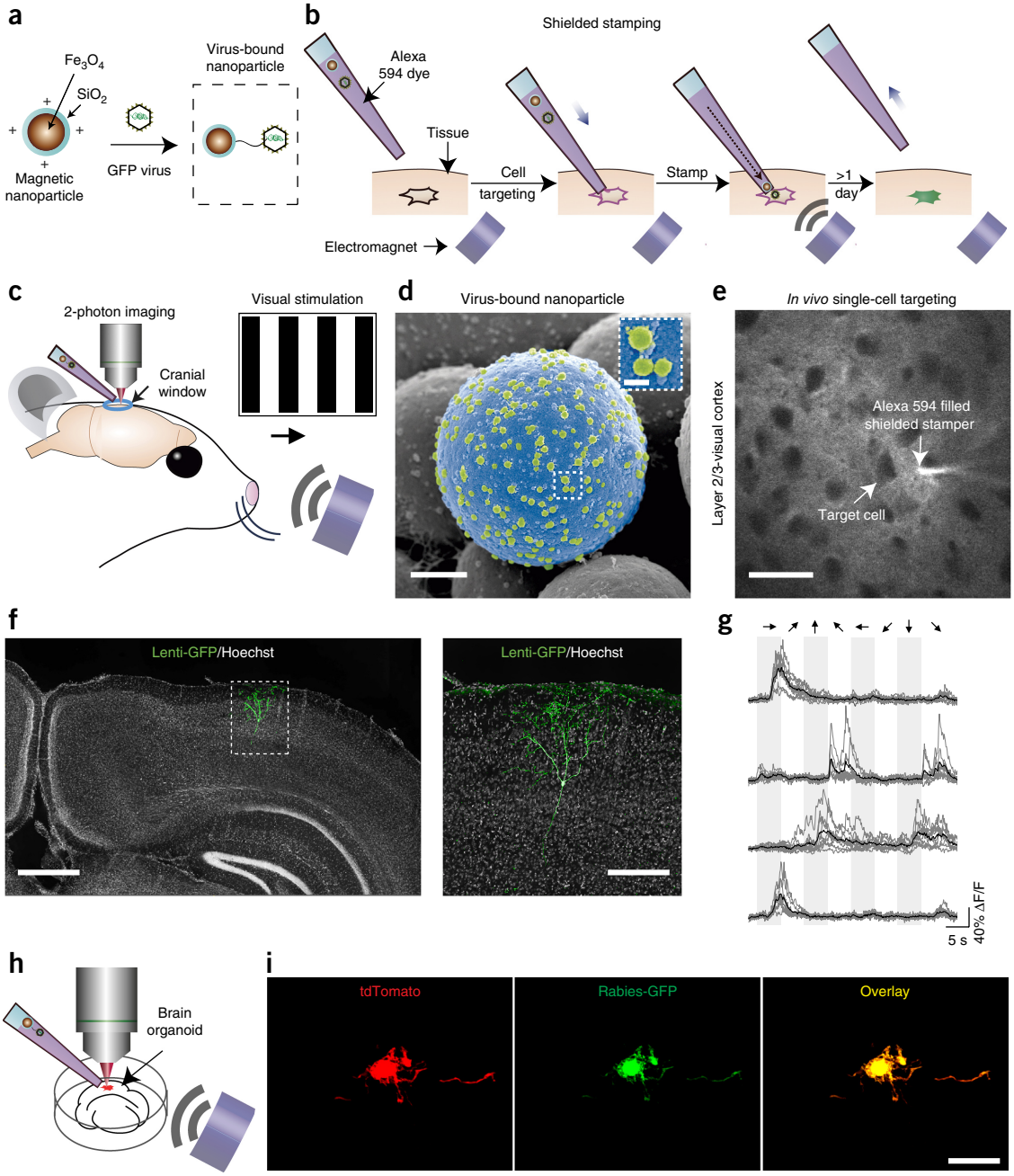

Figure 3 Single-cell virus stamping using a shielded stamper in mouse brain *in vivo* and in human brain organoid. (**a**–**b**) Schematic representation of the key steps. A virus, here encoding *GFP*, is bound to a chemically functionalized magnetic nanoparticle (**a**). A patch pipette containing Alexa 594 dye is back-filled with virus-bound nanoparticles (**b**). The pipette is advanced through tissue and a target cell is located using two-photon-assisted shadow imaging. Once the target cell is reached, the electromagnet is turned on and the magnetic field guides the virus-coated nanoparticles into contact with the cell membrane. After 3–5 min the magnet is turned off, the pipette is removed, and the tissue is monitored for the expression of the fluorescence marker. (**c**) A schematic of the experimental design for shielded virus stamping within the mouse brain. (**d**) SEM of a magnetic nanoparticle (pseudo-colored blue) to which is bound VSVG-coated lenti viruses (pseudo-colored green). Scale bars, 500 nm (overview) and 100 nm (inset). (**e**) Example of single-cell targeting in deep brain tissue using two-photon-assisted shadow imaging. Scale bar, 40 µm. (**f**) A fixed and stained coronal section of mouse visual cortex showing a single GFP-expressing target cell (green) and nuclear staining with Hoechst (white). Left, low-magnification, right, high-magnification image. Scale bars, 200 µm (left) and 80 µm (right). (**g**) Light responses from GCaMP6s-expressing neurons in mouse visual cortex (layer 2/3). Shielded virus stamping was used to deliver magnetic nanoparticles bound with AAVs encoding *GCaMP6s*. Visual stimuli, consisting of gratings drifting in eight different directions were used (gray lines represent individual trials and black lines represent the average of all six trials; each row shows responses from a different neuron). (**h**) Schematic of the experimental design for stamping a single cell in a brain organoid using a shielded stamper and two-photon-assisted target imaging (top left). (**i**) Stamping a single tdTomato-expressing neuron (left) with VSVG-coated rabies viruses encoding *GFP* (middle) in a human brain organoid. The overlay of red and green channels is shown (right). Dashed lines indicate the outer shell of the organoid. Scale bar, 50 µm.

of the target cell by turning on an electromagnet that was aligned with the pipette.

To determine the efficacy and specificity of shielded virus stamping, we first tested it in cell culture. We found that virus-bound nanoparticles pipetted onto cultured HEK293T cells led to robust infection (**Supplementary Fig. 4a–c**). Next, we used fluorescence-activated cell sorting to deliver virus-coated, single nanoparticles to individual wells in a 96-well plate that were plated with HeLa Kyoto cells and found that single nanoparticles were sufficient to infect cells (**Supplementary Fig. 4d–f**). Furthermore, by using a magnet to separate the virus-bound nanoparticles from the solution they were in, we found that the solution became non-infective (**Supplementary Fig. 4g**,**h**). We performed shielded virus stamping by placing the pipette tip next to the soma of a cultured cell of interest and turning on the electromagnet for 3–5 min, before turning the magnet off and retracting the pipette. Using this strategy, we expressed tdTomato, in a targeted manner, exclusively in pre-labeled GFP-expressing cells (**Supplementary Fig. 4i**; $n = 3$).

We then tested shielded virus stamping for infecting single cells within tissue. We performed shielded virus stamping *in vivo* on neurons in layer 2/3 of mouse visual cortex (130–330 µm below the brain surface). In an anesthetized mouse, we opened a cranial window above the visual cortex and positioned an electromagnet in front of the mouse (**Fig. 3c**). The magnet was close to the mouse's nose (~2 cm from the stamping position of pipette tip) and was aligned parallel to the approach angle of the pipette. We filled a patch pipette with solution containing the dye Alexa 594 and back-filled the pipette with VSVG-coated lenti-virus-coated magnetic nanoparticles (**Fig. 3d**). The lenti viruses encoded *GFP*. We inserted the patch pipette into the cortex at an angle of ~45° and advanced it to layer 2/3 using shadow imaging[35] in which fluorescent dye is expelled from the tip of a patch pipette to fill the extracellular space with dye and reveal the cell bodies of nearby neurons, imaged under a two-photon microscope as dark 'shadows' (**Fig. 3e**). Subsequently, the pipette tip was placed adjacent to a cell body and the nanoparticles were pulled into contact with the membrane of the targeted cell by turning on the electromagnet (**Fig. 3b**). The power of the electromagnet, when turned on, was ~100 mTesla at the pipette tip. After 3–5 min, the electromagnet was turned off and the pipette was retracted. The cranial window was then covered with a glass coverslip. The targeted single cell became brightly fluorescent *in vivo* 1–4 d after virus stamping ($n = 6$ infected single cells out of 29 attempts). In some experiments, we removed and sectioned the brain, and assessed GFP expression using immunohistochemistry. GFP fully labeled the cell body and processes of a single cell (**Fig. 3f**).

We performed three experiments to test for possible effects of exposure to the magnetic field and the nanoparticles on the health of cells *in vivo*. First, we used the shielded virus stamper to deliver to the visual cortex magnetic nanoparticles to which we had bound VSVG-coated G-deleted rabies viruses encoding the calcium indicator *GCaMP6s*[36]. Six days after stamping, we detected robust light responses from GCaMP6s-expressing neurons (**Supplementary Fig. 5a**,**b**), including direction- and orientation-selective responses, suggesting that virus-stamped cells and their circuits remained healthy. We also used the shielded virus stamper *in vivo* to deliver magnetic nanoparticles coated with AAVs to drive stable, long-term expression of GCaMP6s in cells in the visual cortex. We recorded robust light responses 18 d after stamping (**Fig. 3g**). Second, we expressed GCaMP6s in mice via systemic injection of a PHP.B serotype AAV[37,38], then examined the responses in the visual cortex to visual stimulation before and immediately after a 10-min exposure to the magnetic field. We found the visually evoked activity profile of all neurons recorded ($n = 36$) to be significantly correlated before and after exposure to the magnetic field (Pearson correlation coefficient = 0.757, $P < 0.001$, **Supplementary Fig. 5c**). Third, we injected magnetic nanoparticles that had not been coated with viruses into the cortex of mice that expressed GCaMP6s via systemic AAV delivery. A week after the nanoparticles were injected, we recorded robust light responses in the visual cortex (**Supplementary Fig. 5d**).

To better understand how the magnet affects the magnetic nanoparticles within the shielded stamper, we simulated the magnetic field created by the electromagnet (**Supplementary Note 1** and **Supplementary Fig. 6a–c**). Experimentally measuring the strength of the magnetic field confirmed that the simulated values were realistic (coefficient of determination = 0.984, **Supplementary Fig. 6b**). In our experiment, the strength of the magnetic field created by the electromagnet could be adjusted via the electric current and by changing the distance and the tilting of the magnet relative to glass pipette and sample (**Supplementary Fig. 6a**). We examined fluorescently labeled nanoparticles dispersing from a pipette tip onto a cell culture sample. We found that cell surfaces contained fluorescently labeled areas of different sizes, suggesting that both mono-dispersed and aggregated nanoparticles were present in the pipette used for shielded virus stamping (**Supplementary Fig. 6d**).

Finally, we performed shielded stamping within tissue in human brain organoids. The organoids were developed from human induced pluripotent stem cells[39]. We targeted individual cells using the two-photon-assisted shadow-imaging strategy (50–150 µm below organoid surface), as described above[35], and performed shielded virus stamping of individual organoid cells with VSVG-coated G-deleted rabies viruses encoding *GFP*. We then incubated organoids and after 3–5 d we found individual cells expressing GFP ($n = 5$ infected single cells out of 20 attempts). We then tested whether shielded virus stamping could be used to target infection to pre-selected cells within tissue. We electroporated brain organoids with plasmid encoding *tdTomato* to allow for sparse transfection, then used two-photon-assisted single-cell targeting to perform shielded virus stamping on individual tdTomato-expressing cells with VSVG-coated G-deleted rabies encoding *GFP*. 3–5 d after stamping we found individual cells co-expressing GFP and tdTomato (**Fig. 3h**,**i**; $n = 2$ double-labeled single cells out of 20 attempts).

DISCUSSION

Virus stamping involves reversibly binding viruses to a delivery vehicle that is then brought into contact with a single target cell. By concentrating virus particles on the delivery vehicle, it allows use of viruses at a lower titer than usually required for single-cell infection (**Supplementary Fig. 7**). This is particularly advantageous because manufacturing enveloped viruses at high titer requires specialized expertise. Furthermore, since virus stamping allows for the delivery of viral particles exclusively to a single cell body, it should reduce immune responses that can happen concomitantly with standard virus injection procedures[40].

Beyond the applications presented here, virus stamping could also be useful in addressing questions in general virology, such as assessing receptor distribution on polarized cells, identifying permissive cells in complex organs, and studying receptor–virus interaction and viral entry[41].

In our experiments, we used two-photon-assisted shadow imaging to target cells for virus stamping. This approach limited our ability to stamp to the visible range for standard two-photon imaging (<1 mm deep in tissue). In the future, it may be possible to combine

virus stamping with blind cell-attached electrophysiological recordings or channel rhodopsin-assisted patching[42] to allow for targeting of cells deeper in tissue.

Considering that currently the success rate of *in vivo* single-cell virus stamping is ~20%, in some applications stochastic labeling of cells using sparse bulk infection may be preferred. For instance, stochastic labeling may be preferred for discovering the physiological and morphological diversity of a brain region. Virus stamping may be advantageous in several settings, such as single-cell-initiated virus tracing and genetic engineering of a population of cells with known physiology but no genetic access. In this latter case, cells could be characterized first using cellular resolution functional imaging, followed by virus stamping different members of a functionally similar group. By stamping more than one cell per brain area, it is also possible to increase the success rate well above 20%. Finally, virus stamping should enable genetically engineering a single cell with multiple genetic additions, which could require infecting a single cell with multiple viruses, either simultaneously or at different time points.

Future developments in which virus is bound to magnetic nanoparticles and the nanoparticles are coated with biodegradable polymers or are made to be photo-uncageable could enable bulk, remote-controlled virus stamping. For example, when injected into the blood, magnetic nanoparticles with bound virus could be forced to cross the blood–brain barrier, via magnetic attraction, at specified locations to cause infection of a chosen brain region. Alternatively, when deposited on the surface of the brain, virus-coated magnetic nanoparticles could be magnetically steered to specified deep brain regions.

METHODS

Methods, including statements of data availability and any associated accession codes and references, are available in the online version of the paper.

Note: Any Supplementary Information and Source Data files are available in the online version of the paper.

ACKNOWLEDGMENTS

We thank J. Gründemann for technical assistance setting up the brain slice procedure, J.M. Mateos, A. Kaech, and J. Doehner from the Zurich Center of Microscopy and Image Analysis (ZMB), U. Schwarz from Leica Mannheim, and T. Horn from the DBSSE imaging facility for helping with imaging and data preparation, M.J. Schnell for providing the BSR-VSV-RVG cell line, E.M. Callaway for providing the B7GG cell line, C.P. Patino Alvarez and A. Villemain for producing viruses, Helbling Technik Bern AG for technical assistance modeling the magnet used for shielded virus stamping, and the members of the Roska laboratory for technical assistance. The study was supported by a European Union grant (FP7/211800) to D.J.M.; a Human Frontier Science Program Long-Term Fellowship (LT000173/2013-L) and a Swiss National Science Foundation Ambizione Fellowship to S.T.; a European Molecular Biology Organization Long-Term Fellowship (506-2012) to D.M.M.; Swiss National Science Foundation grants (310030B_160225 to D.J.M. and 3100330B_163457 to B.R.), the National Center of Competence in Research Molecular Systems Engineering grant to D.J.M. and B.R.; European Research Council (669157, RETMUS), DARPA (HR0011-17-C-0038, Cortical Sight) grants to B.R., a Deutsche Forschungsgemeinschaft grant (SFB870) to K.K.C.

AUTHOR CONTRIBUTIONS

Experiments were designed by R.S., S.T., K.B., G.K., G.F., D.J.M., and B.R. G-deleted rabies variants were made by A.G. and K.K.C. Cell cultures, immunohistochemistry, electron microscopy, and confocal microscopy were performed by R.S. with the exception of *in vivo* samples, which were processed by A.W., and organoid samples, which were processed by M.M. Viruses were prepared by R.S., K.B., M.A.M., R.N., and K.Y. Pipettes for unshielded virus stamping were prepared by D.M.M. Brain slice preparations, retinal preparations, unshielded virus stamping, and tissue cultures were performed by S.T. and K.B. The magnetic forces related to the magnet used for shielded stamping were measured and modeled by R.S. and C.S.C. Sequential multi-day single-cell infection experiments were performed by R.S. and C.S.C. Magnetic nanoparticle preparations and shielded stamping in cell culture were performed by R.S. *In vivo* nanoparticle optimization was performed by D.H. Shielded *in vivo* stamping was performed by S.T. and G.K. Organoids were grown by M.M., J.K., and B.G.S. Shielded organoid stamping was performed by G.K. and M.M. *In vivo* two-photon calcium imaging was performed by G.K. Computer reconstructions were performed by R.S., M.A.M., and A.P. Figures were made by R.S., S.T., M.M., and G.K. The paper was written by R.S., S.T., D.J.M., and B.R.

COMPETING FINANCIAL INTERESTS

The authors declare competing financial interests: details are available in the online version of the paper.

1. Callaway, E.M. Transneuronal circuit tracing with neurotropic viruses. *Curr. Opin. Neurobiol.* **18**, 617–623 (2008).
2. Hsu, P.D., Lander, E.S. & Zhang, F. Development and applications of CRISPR-Cas9 for genome engineering. *Cell* **157**, 1262–1278 (2014).
3. Swiech, L. *et al.* In vivo interrogation of gene function in the mammalian brain using CRISPR-Cas9. *Nat. Biotechnol.* **33**, 102–106 (2015).
4. Marshel, J.H., Mori, T., Nielsen, K.J. & Callaway, E.M. Targeting single neuronal networks for gene expression and cell labeling in vivo. *Neuron* **67**, 562–574 (2010).
5. Rancz, E.A. *et al.* Transfection via whole-cell recording in vivo: bridging single-cell physiology, genetics and connectomics. *Nat. Neurosci.* **14**, 527–532 (2011).
6. Wertz, A. *et al.* PRESYNAPTIC NETWORKS. Single-cell-initiated monosynaptic tracing reveals layer-specific cortical network modules. *Science* **349**, 70–74 (2015).
7. Fishell, G. & Heintz, N. The neuron identity problem: form meets function. *Neuron* **80**, 602–612 (2013).
8. Siegert, S. *et al.* Genetic address book for retinal cell types. *Nat. Neurosci.* **12**, 1197–1204 (2009).
9. Belgard, T.G. *et al.* A transcriptomic atlas of mouse neocortical layers. *Neuron* **71**, 605–616 (2011).
10. Bernard, A. *et al.* Transcriptional architecture of the primate neocortex. *Neuron* **73**, 1083–1099 (2012).
11. Turner, D.L. & Cepko, C.L. A common progenitor for neurons and glia persists in rat retina late in development. *Nature* **328**, 131–136 (1987).
12. Walsh, C. & Cepko, C.L. Clonally related cortical cells show several migration patterns. *Science* **241**, 1342–1345 (1988).
13. Eiraku, M. *et al.* Self-organizing optic-cup morphogenesis in three-dimensional culture. *Nature* **472**, 51–56 (2011).
14. Kadoshima, T. *et al.* Self-organization of axial polarity, inside-out layer pattern, and species-specific progenitor dynamics in human ES cell-derived neocortex. *Proc. Natl. Acad. Sci. USA* **110**, 20284–20289 (2013).
15. Lancaster, M.A. & Knoblich, J.A. Organogenesis in a dish: modeling development and disease using organoid technologies. *Science* **345**, 1247125 (2014).
16. Vélez-Fort, M. *et al.* The stimulus selectivity and connectivity of layer six principal cells reveals cortical microcircuits underlying visual processing. *Neuron* **83**, 1431–1443 (2014).
17. Stiefel, P. *et al.* Cooperative vaccinia infection demonstrated at the single-cell level using FluidFM. *Nano Lett.* **12**, 4219–4227 (2012).
18. Martínez-Martín, D. *et al.* Inertial picobalance reveals fast mass fluctuations in mammalian cells. *Nature* **550**, 500–505 (2017).
19. Nguyen, T.D. *et al.* Targeted single-neuron infection with rabies virus for transneuronal multisynaptic tracing. *J. Neurosci. Methods* **209**, 367–370 (2012).
20. Cronin, J., Zhang, X.-Y. & Reiser, J. Altering the tropism of lentiviral vectors through pseudotyping. *Curr. Gene Ther.* **5**, 387–398 (2005).
21. Wickersham, I.R., Sullivan, H.A. & Seung, H.S. Axonal and subcellular labelling using modified rabies viral vectors. *Nat. Commun.* **4**, 2332 (2013).
22. Haberl, M.G. *et al.* An anterograde rabies virus vector for high-resolution large-scale reconstruction of 3D neuron morphology. *Brain Struct. Funct.* **220**, 1369–1379 (2015).
23. Mothes, W., Sherer, N.M., Jin, J. & Zhong, P. Virus cell-to-cell transmission. *J. Virol.* **84**, 8360–8368 (2010).
24. Burns, J.C., Friedmann, T., Driever, W., Burrascano, M. & Yee, J.K. Vesicular stomatitis virus G glycoprotein pseudotyped retroviral vectors: concentration to very high titer and efficient gene transfer into mammalian and nonmammalian cells. *Proc. Natl. Acad. Sci. USA* **90**, 8033–8037 (1993).
25. Carneiro, F.A., Bianconi, M.L., Weissmüller, G., Stauffer, F. & Da Poian, A.T. Membrane recognition by vesicular stomatitis virus involves enthalpy-driven protein-lipid interactions. *J. Virol.* **76**, 3756–3764 (2002).
26. Conti, C., Mastromarino, P., Riccioli, A. & Orsi, N. Electrostatic interactions in the early events of VSV infection. *Res. Virol.* **142**, 17–24 (1991).
27. Bailey, S.N., Ali, S.M., Carpenter, A.E., Higgins, C.O. & Sabatini, D.M. Microarrays of lentiviruses for gene function screens in immortalized and primary cells. *Nat. Methods* **3**, 117–122 (2006).
28. Lei, P., Bajaj, B. & Andreadis, S.T. Retrovirus-associated heparan sulfate mediates immobilization and gene transfer on recombinant fibronectin. *J. Virol.* **76**, 8722–8728 (2002).

29. Wegmann, F. *et al.* Polyethyleneimine is a potent mucosal adjuvant for viral glycoprotein antigens. *Nat. Biotechnol.* **30**, 883–888 (2012).
30. Nakagawa, T. *et al.* Fabrication of amino silane-coated microchip for DNA extraction from whole blood. *J. Biotechnol.* **116**, 105–111 (2005).
31. Hunt, L.A. & Summers, D.F. Glycosylation of vesicular stomatitis virus glycoprotein in virus-infected HeLa cells. *J. Virol.* **20**, 646–657 (1976).
32. Elaissari, A. *Colloidal Biomolecules, Biomaterials, and Biomedical Applications* (CRC Press, 2003).
33. Barde, I., Salmon, P. & Trono, D. Production and titration of lentiviral vectors. **53**, 4.21 *Curr. Protoc. Neurosci.* (2010).
34. Hatori, M. *et al.* Inducible ablation of melanopsin-expressing retinal ganglion cells reveals their central role in non-image forming visual responses. *PLoS One* **3**, e2451 (2008).
35. Judkewitz, B., Rizzi, M., Kitamura, K. & Häusser, M. Targeted single-cell electroporation of mammalian neurons in vivo. *Nat. Protoc.* **4**, 862–869 (2009).
36. Chen, T.-W. *et al.* Ultrasensitive fluorescent proteins for imaging neuronal activity. *Nature* **499**, 295–300 (2013).
37. Deverman, B.E. *et al.* Cre-dependent selection yields AAV variants for widespread gene transfer to the adult brain. *Nat. Biotechnol.* **34**, 204–209 (2016).
38. Hillier, D. *et al.* Causal evidence for retina-dependent and -independent visual motion computations in mouse cortex. *Nat. Neurosci.* **20**, 960–968 (2017).
39. Lancaster, M.A. *et al.* Cerebral organoids model human brain development and microcephaly. *Nature* **501**, 373–379 (2013).
40. Drokhlyansky, E. *et al.* The brain parenchyma has a type I interferon response that can limit virus spread. *Proc. Natl. Acad. Sci. USA* **114**, E95–E104 (2017).
41. Alsteens, D. *et al.* Nanomechanical mapping of first binding steps of a virus to animal cells. *Nat. Nanotechnol.* **12**, 177–183 (2017).
42. Muñoz, W., Tremblay, R. & Rudy, B. Channelrhodopsin-assisted patching: in vivo recording of genetically and morphologically identified neurons throughout the brain. *Cell Reports* **9**, 2304–2316 (2014).

ONLINE METHODS

Reagents. Unless otherwise noted, all reagents were purchased from Sigma-Aldrich.

Cell lines. HeLa Kyoto (Gibco-Life technologies, NY, USA), HEK 293T (HEK EcR-293; Invitrogen), BHK-21 (ATCC, CCL-10), BSR-VSV-RVG (provided by M. Schnell) and BHK- B7GG (provided by E.M. Callaway) cells all tested negative for mycoplasma using a mycoplasma detection kit (ATCC, 30-1012K, USA) (see **Life Sciences Reporting Summary**).

Production of VSVG-coated G-deleted rabies virus. SADΔG-*GFP* rabies virus (referred to in the text as G-deleted rabies virus encoding *GFP*) has been described previously[43]. To obtain SADΔG-*ChR2C128T-2A-tdTomato* (referred to in the text as G-deleted rabies virus encoding *tdTomato*), we replaced the rabies-G open reading frame with *ChR2C128T-2A-tdTomato*. G-deleted rabies viruses encoding *BFP* and *YFP* were obtained similarly. Both SADΔG-*GFP* and SADΔG-*ChR2C128T*-2A-*tdTomato* rabies viruses were amplified, and concentrated by ultracentrifugation, as described previously[44] with the following modifications: at the amplification step we used the B7GG cell line instead of the BHK-B19G2 cell line. Next, in order to coat the virus particles with VSVG glycoprotein, rabies viruses were propagated on a BSR-VSV-RVG cell line[45]. Next, we performed the ultracentrifugation step and, at the end of the ultracentrifugation, the supernatant was discarded and 100 µl NTE solution (100 mM NaCl, 10 mM TRIS HCl, 1 mM EDTA, pH 7.5) was added to the pellet. After 5-min incubation at room temperature, the pellet was resuspended using gentle trituration. Viral stocks were kept in 20-µl aliquots at −80 °C. For each experiment, freshly thawed rabies virus was used. For titration, we used BHK-21 cells plated in six-well plates. From each batch of virus one aliquot was thawed and mixed with 280 µl DMEM supplemented with 1 mM sodium pyruvate, 1% FBS (FBS) and 1% penicillin/streptomycin. From this mixture, a serial tenfold dilution was generated with culture medium up to 5 log dilutions, where each dilution had a final volume of 300 µl. These were then added to the wells and incubated for 1 h at 37 °C and 5% CO_2. Then 1.5 ml culture medium was added and incubated for 48 h until the infected cells developed bright fluorescence. Titer was determined by manual counting of the fluorescently labeled cells under fluorescent microscope. The titer was higher than 10^7 infectious particles/ml.

Production of VSVG-coated lenti virus. To obtain replication-deficient lenti virus (LV) encoding *GFP*, we first replaced the hPGK promoter in the pRRLSIN.cPPT.PGK-*GFP*.WPRE plasmid (Addgene, #12252) with an EF1a promoter, yielding the pLV-*eGFP* plasmid. Lenti virus encoding *tdTomato* was obtained similarly. In order to make LV-encoding *rabies-G* of the challenge virus standard 11 rabies strain (CVS11G), we replaced the *GFP* gene with the gene encoding *CVS11G*[46], yielding pLV-*CVS11G*. Together with the helper plasmids pCMVR8.74 (Addgene, #22036) and pMD2.G (Addgene, #12259), these plasmids were used for virus production in HEK293T cells. After transfection, the production medium was changed to serum-free Episerf (Gibco). Apart from this change, the lenti virus production was carried out as previously described[33]. Titers of GFP-encoding lenti virus were determined via a dilution series on 293T cells and subsequent flow cytometric quantification. For rabies-G encoding lenti virus, qPCR titration (using Applied Biosystems, TaqMan reagents) was performed as previously described[33]. In both cases the titers were higher than 10^6 infectious particles/ml.

HSV and AAV production. HSVs were obtained from R. Naeve (MIT vector core). AAVs were made in-house using standard protocols.

Animals. All animal experiments and procedures were performed in accordance with standard ethical guidelines (European Communities Guidelines on the Care and Use of Laboratory Animals, 86/609/EEC) and were approved by the Veterinary Department of the Canton of Basel-Stadt. Animals were maintained under a 12 h light-dark cycle. Brain slices and retinae were obtained from, and *in vivo* experiments were performed with, 4- to 8week old female C57Bl/6J mice (Charles River Laboratories). Retinae with tdTomato expression in melanopsin-positive ganglion cells were obtained from ~1-year-old male and female mice bred by crossing *Opn4*-Cre mice[34] with tdTomato-expressing Ai9 mice[47]. Cortical neuron cultures were obtained from Wistar rats[48].

Cell culture. HEK293T, BHK and HeLa Kyoto cells were passaged under 5% CO_2 at 36 °C in DMEM adjusted with 4 mM L-glutamine, 1.5 g/l sodium bicarbonate, 4.5 g/l glucose, 10% bovine calf serum, and 1% penicillin/streptomycin. HEK293T and BHK cells with a density of 10^5 cells/ml were plated on 18-mm glass coverslips (VWR International) and grown until they reached 80% confluence; they were then used for experiments. For HeLa Kyoto cell plating see FACS method section below. For virus stamping experiments, coverslips containing BHK cells were perfused with DMEM supplemented with 10% FCS that was bubbled with 95% O_2 and 5% CO_2 at 36 °C.

Cortical neuron culture. Embryonic day 18 rat cortical neuron cultures were obtained as described before[48]. Briefly, the plating medium consisted of 850 µl neurobasal medium (Gibco), supplemented with 10% horse serum (HyClone), 0.5 mM GlutaMAX (Invitrogen), and 2% B-27 (Invitrogen). After 24 h, the plating medium was changed to growth medium: 850 µl DMEM (Invitrogen), supplemented with 10% horse serum, 0.5 mM GlutaMAX, and 1 mM sodium pyruvate (Invitrogen). Cultures were matured for 1 week in a gas-controlled incubator (5% CO_2, Thermo Scientific) before experimentation. For virus stamping experiments, coverslips containing cortical neurons were perfused with DMEM with 10% FCS and bubbled with 95% O_2 and 5% CO_2 at 36 °C. Transfection of cortical neurons with GFP was performed using Lipofectamin (Invitrogen).

Retina preparation. After mice had been euthanized, the eyes were removed and retinae were dissected in warm Ringer's solution (110 mM NaCl, 2.5 mM KCl, 1 mM $CaCl_2$, 1.6 mM $MgCl_2$, 10 mM glucose, 22 mM $NaHCO_3$). The isolated retina was subsequently mounted ganglion cell side up on a membrane filter (Millipore) with a 2 × 2 mm pre-cut window, allowing light from the microscope to reach the retina and enabling the preparation to be viewed under the microscope. For stamping experiments, the isolated retina was then perfused with heated Ringer's solution (36 °C) that was bubbled with 95% O_2 and 5% CO_2. To allow access to ganglion and amacrine cell bodies, a 5–10 MΩ pipette filled with Ringer's solution was used to tear a hole in the inner limiting membrane.

Brain sectioning. After mice were euthanized, brains were immediately removed and transferred to ice-cold artificial cerebral spinal fluid (ACSF, 124 mM NaCl, 1.25 mM NaH_2PO_4, 2.7 mM KCl, 26 mM $NaHCO_3$, 1.3 mM $MgCl_2$, 2 mM $CaCl_2$, 18 mM glucose) that had been bubbled with 95% O_2 and 5% CO_2. The cerebellum was removed with a scalpel and the caudal portion of the brain was glued onto the base of a vibratome (Leica VT1200S). Next, 150- to 200-µm thick brain slices were cut and transferred to a chamber containing ACSF that had been bubbled with 95% O_2 and 5% CO_2 (only cortical sections were collected) and kept at 36 °C for 30 min before being used for virus stamping. For virus stamping experiments, brain slices were perfused with heated (36 °C) and bubbled ACSF and fixed in place in the chamber with a custom-made harp.

Glass pipette preparation. A detailed step-by-step methodology for preparing pipettes for unshielded virus stamping is provided below:

Step 1. Pulling and blunting pipettes (**Supplementary Fig. 1a**).

(i) Patch pipettes with a resistance of ~10 MΩ were pulled on a P-97 Flaming/Brown pipette puller (Sutter Instruments), using glass capillaries with 1-mm outer diameter and 0.5-mm inner diameter (Sutter Instruments).

(ii) Pipettes were flame-blunted using a Bunsen burner (Laborbedarf AG) and mounted in a custom-made Teflon holder.

(iii) The pipette tips were assessed for proper morphology (i.e., a small, smooth, unbroken tip as shown in **Fig. 1d**,**g** and **Supplementary Fig. 1f** under a bench-top microscope (Nikon)).

Step 2. Cleaning of pipettes[49] (**Supplementary Fig. 1b**).

(i) 35 g KOH was dissolved in 35-ml ultrapure water (Thermo Fisher Scientific). This reaction was performed in a staining jar (Fischer Scientific). Once the KOH had been dissolved, 300 ml pure ethanol was added, yielding a solution of ethanolic potassium hydroxide.

(ii) The Teflon holder, together with the pipettes, was immersed in the ethanolic potassium hydroxide in the staining jar and sonicated at 25 kHz for 5 min at room temperature in an ultrasonicator water bath (VWR).

(iii) Following sonication, the ethanolic potassium hydroxide solution was replaced with 300 ml ultrapure water. The pipettes were then sonicated in ultrapure water at 25 kHz for 5 min at room temperature. This washing step was repeated three times.

Step 3. Silane functionalization of pipettes (**Supplementary Fig. 1c**).

(i) The functionalization solution was made by adding 300 µl AEEA (Sigma Cat No. 413348) to 300 ml ultrapure water in a staining jar.

(ii) Cleaned pipettes were placed into the functionalization solution and rocked gently on a shaker (VWR) for 15 min (30 oscillations per min).

(iii) The pipettes were removed from the functionalization solution and submerged for 5 s in a new staining jar containing 300 ml pure 100% isopropanol.

(iv) The pipettes were placed into a fresh jar containing 300 ml ultrapure water and sonicated at 25 kHz for 5 min. This step was repeated two more times.

(v) The pipettes were transferred to an oven (VWR) and fully dried at 65 °C for 2 h.

(vi) The tip morphology of AEEA-coated pipettes was checked again under the microscope and stored on a pre-polymerized PDMS (polydimethylsiloxane)-coated Petri dish for up to 24 h until the virus binding step was performed.

Step 4. Virus binding to pipettes (**Supplementary Fig. 1d**).

(i) A mixture of 20 µl virus aliquot and 10 µl NTE was prepared and was placed onto an 18-mm coverslip positioned near an edge in a PDMS-coated Petri dish.

(ii) Two to four pipettes were carefully placed in the Petri dish, with their tips submerged in the virus solution on the coverslip. A folded, wet Kimwipe (Kimberly-Clark International) was placed in the Petri dish to prevent drying out of the viral solution during the incubation period. The lid of the Petri dish was then sealed with parafilm and incubated for 1 h at 4 °C.

(iii) After incubation, pipettes were gently washed three times by aspirating away virus solution and replacing it with 50 µl L-15 medium (Sigma). After washing, pipette tips were left in 50 µl L-15 before being used for virus stamping.

Virus stamping of surface cells. Virus-bound pipettes were transferred to the solution that was used to perfuse the cells or tissues. The pipette tip and the cells or tissue were imaged with an EM-CC C9100 (Hamamatsu) or a Spot RTKE (Diagnostic Instruments) CCD camera, attached to an upright Nikon Eclipse E600FN microscope (Nikon) fitted with a 60× water immersion lens (NA 1.0, Nikon). Microscope light was filtered with an IR filter and passed through the sub-stage condenser, which was used to focus the light onto the cells or tissue. For targeting fluorescent cells for virus stamping, the IR image was combined with a fluorescent image using a two-photon laser scanning microscope system[50]. The pipette tip was then positioned such that it lightly touched the cell body of the target cell (**Supplementary Fig. 1f**). The pipette tip was held against the cell for 1 min while ensuring that physical disturbances were kept to a minimum. The pipette was then removed from the solution and the cells or tissue were cultured.

Cell and tissue culturing after virus stamping surface cells. After virus stamping, the cells, brain slices or retinae were transferred to a heated (36 °C) and gas-controlled (5% CO_2) incubator. Cell and cortical neuron cultures were incubated in the same culture medium as indicated above for 1–2 d. Retinae and brain slices were cultured on Millicell cell culture inserts (Millipore) in six-well plates. Retinae were cultured for up to 6 d in DMEM supplemented with 10% horse serum. Brain slices were cultured for up to 6 d in medium previously developed for hippocampal cultures[51]. For both retina and brain slices, the culture medium was changed every second day. Cell and tissue cultures were assessed for viral infection via fluorescent protein expression using an epi-fluorescence microscope (Olympus SZX16) equipped with an X-Cite120 PC Q light source (Scientifica).

Immunohistochemistry. Cultured cells were fixed in 4% (w/v) paraformaldehyde (PFA) in PBS (137 mM NaCl, 2.7 mM KCl, 4.3 mM Na_2HPO_4, 1.47 mM KH_2PO_4, pH 7.4) for 5 min and subsequently washed three times with PBS. Next, cells were blocked for 1 h in 10% (w/v) normal donkey serum (NDS; Chemicon), 1% (w/v) bovine serum albumin (BSA), and 0.5% (v/v) Triton X-100 in PBS. Primary antibodies were incubated for 1 h in 3% (v/v) NDS, 1% (w/v) BSA, 0.02% (w/v) sodium azide, and 0.5% (v/v) Triton X-100 in PBS, followed by an overnight wash. Secondary antibodies were incubated for 30 min in 3% (v/v) NDS, 1% (w/v) BSA, and 0.5% (v/v) Triton X-100. After a final wash in PBS, cells were embedded in Prolong Gold antifade (Invitrogen).

Retinae were fixed for 30 min in 4% PFA and then washed with PBS for at least 1 d at 4 °C. To aid penetration of the antibodies, retinae were frozen and thawed three times with 30% (w/v) sucrose in PBS. All other procedures were carried out at room temperature. After washing in PBS, retinae were blocked for 1 h in 10% NDS, 1% BSA, and 0.5% Triton X-100 in PBS. Primary antibodies were incubated for 7d in 3% NDS, 1% BSA, 0.02% sodium azide, and 0.5% Triton X-100 in PBS, followed by an overnight wash. Secondary antibodies were incubated for 2 h in 3% NDS, 1% BSA, and 0.5% Triton X-100 in PBS together with DAPI (4′,6-diamidine-2-phenylindole dihydrochloride, Roche Diagnostics, 10 µg/ml) to label cell nuclei. After a final wash in PBS, retinae were mounted on glass slides and embedded in Prolong Gold.

Brain slice cultures were fixed for 30 min in 4% PFA in PBS and then washed with PBS for 5 min at 4 °C, followed by incubation in 20% (w/v) methanol in PBS for 5 min. Next, slices were washed three times in PBS for 5 min. Slices were then permeabilized in 0.5% Triton X-100 in PBS for 12 h at 4 °C. Slices were then blocked for 1 h in 10% NDS, 1% BSA, and 0.5% Triton X-100 in PBS. Primary antibodies were incubated overnight in 3% NDS, 1% BSA, 0.02% sodium azide, and 0.5% Triton X-100 in PBS, followed by an overnight wash. Secondary antibodies were incubated for 2 h in 3% NDS, 1% BSA, and 0.5% Triton X-100 in PBS together with DAPI. After a final wash in PBS, brain slices were mounted on glass slides and embedded in Prolong Gold.

For *in vivo* (deep tissue stamping) experiments, whole brains were removed and fixed overnight in 4% PFA in PBS. Coronal sections (150 µm thick) were made with a vibratome and slices were then processed as previously described[6]. For brain organoid stamping experiments, organoids were fixed overnight in 4% PFA, and sliced in 150-µm thick slices.

The following primary and secondary antibody combinations were used. (1) Primary: goat anti-ChAT (1:200, AB144P, Chemicon). Secondary: donkey anti-goat IgG conjugated with Alexa Fluor 633 (1:200, A-21082, Invitrogen); (2) primary: rabbit anti-green fluorescent protein (GFP; 1:200, AB3216, Chemicon). Secondary: donkey anti-rabbit IgG conjugated with Alexa 488 (1:200, 711-545-152, Jackson ImmunoResearch); (3) primary: chicken anti-RFP (1:200, AB3528, Millipore). Secondary: donkey anti-chicken IgG conjugated with Cy3 (1:200, 703-165-155, Jackson); (4) primary: mouse anti-rabies glycoprotein (1:200, AB82460, Abcam). Secondary: donkey anti-mouse protein conjugated with Alexa 647 (1:200, A31571, Invitrogen).

Confocal microscopy. Stained cells and tissues were imaged with a Leica SP8 confocal microscope (Leica). Within a given sample, all images were recorded at the same laser power and gain control. Images were acquired with either a 10× lens (NA 0.3) or with a 63× oil immersion lens (NA 1.40).

Scanning electron microscopy. Pipettes/nanoparticles coupled to viruses were fixed in 2.5% glutaraldehyde in PBS for 5 min at room temperature. Fixative was then removed and pipettes/nanoparticles were rinsed gently in PBS three times for 5 min. The pipettes/nanoparticles were then placed in distilled water and subsequently in 1% (w/v) osmium tetroxide (in distilled water) for 1 h at room temperature. Afterwards, the pipettes/nanoparticles were rinsed once more with distilled water and allowed to dehydrate using a graded ethanol series of 30%, 50%, 70%, 90% and, finally, 100% (v/v, 10 min for each step). The pipettes/nanoparticles were left submerged in 100% EtOH and dried using a critical point dryer (Denton, DCP-1). Dried pipettes/nanoparticles were fixed on a custom-made pipette holder and sputter-coated, with either platinum (for VSVG-coated rabies viruses) or a 4:1 gold:palladium mix (for VSVG-coated lenti viruses) for 60 s, using an Ace200 low vacuum coater (Leica). Viruses coating the pipettes/nanoparticles were then imaged using a Zeiss 1550 field-emission scanning electron microscope at 3–5 kV, after the location of the viruses had been identified on a finder grid.

Image analysis. 2D maximum intensity projections were computed using Imaris (Bitplane). Images were deconvolved using Huygens Core software

doi:10.1038/nbt.4034

(Scientific Volume Imaging B.V.). 3D computer reconstructions of dendrites were made using the filament tracer module in Imaris (Bitplane). Reconstructed dendrites were analyzed for contact points between processes using a custom MATLAB (Mathworks) code. To quantify the amount of bound virus particles SEM images were analyzed using the spot detection tool in Imaris. The SEM images could be used directly with a size filter set between 50–120 nm to differentiate viruses from the background. Size distribution analysis of nanoparticles were acquired using the transmission electron microscope and analyzed using the open source software FIJI.

Binding viruses to magnetic nanoparticles. For shielded virus stamping experiments, we bound viruses to magnetic nanoparticles that were comprised of a silica shell and an iron core that were on average 72 nm diameter (Super Mag Silica Beads, SS0051, Alpha Biobeads, USA) or 80 nm (*in vivo* ViroMag, IV-VM30250, OZ Biosciences, France) in size. For scanning electron microscopy imaging and FACS sorting experiments it was necessary to use larger (1–3 µm diameter) magnetic nanoparticles (PMSI-1.5, Kisker, Germany). For nanoparticles from Alpha Biobeads and Kisker, we chemically functionalized them with AEEA by first cleaning the nanoparticles by immersion in sulfuric acid for 5 min, then rinsing them in de-ionized water by holding them in a 1.5-ml centrifuge tube with a permanent magnet (Supermagnete, Switzerland) and drying them overnight under vacuum while they were held down by a permanent magnet. Nanoparticles were then silanized overnight with AEEA in 1% (v/v) toluene (Sigma). Silane solution was then removed and nanoparticles were rinsed with toluene, followed by methanol and finally with de-ionized water. Nanoparticles were then dried under vacuum and were ready of virus binding. For nanoparticles from OZ Biosciences, we did not coat this with AEEA as they were commercially chemically functionalized with a cationic coating.

To bind viruses, we mixed the nanoparticle solution 1:1 with the virus stock solution (the titer of the stocks used was 10^6–10^7 plaque-forming units per ml). For ViroMag nanoparticles, the mixture was incubated for 15 min at room temperature in a 1.5-ml centrifuge tube. For Alpha BioBeads nanoparticles, the mixture was incubated overnight at 4 °C in a 1.5 ml centrifuge tube. Non-functionalized viruses were washed away from the supernatant by pulling down nanoparticles with a permanent magnet (Supermagnete, Switzerland), removing the supernatant and then resuspending the nanoparticles in 100 µl of L-15 media.

Fluorescence-activated cell sorting (FACS) of fluorescent virus-bound nanoparticles. To allow for AEEA-coated nanoparticles to be fluorescently sorted, 10 µl of nanoparticle solution was mixed with 1 µl of Alexa Fluor 488 NHS Ester (ThermoFischer) and 50 µl of PBS for 5 min in a 1.5-ml centrifuge tube. The nanoparticles were then held down with a permanent magnet, the solution was removed and the nanoparticles were washed three times with PBS and then lenti-viruses encoding *tdTomato* were bound (see above). HeLa Kyoto cells were trypsinized, and 1×10^4 cells were seeded on glass-bottomed 96-well plates. The cells were left to culture at 5% CO_2 and 36 °C in DMEM with 10% FCS overnight and allowed to spread and adhere. The following morning, a 50 µl aliquot of virus-bound nanoparticles in PBS was analyzed using a BD LSRFortessa cell analyzer. The Alexa dye was excited with a 488 nm laser and emitted light was filtered with a 530/30 band-pass filter and 505 long-pass mirror. Following gating to select for single nanoparticles, fluorescence intensities of at least 15,000 nanoparticles were recorded, the brightest of these nanoparticles were selected and single nanoparticles were dropped into each well of a 96-well plate. The cultures were then incubated at 5% CO_2 at 36 °C in DMEM with 10% FCS for 24 h and assessed for tdTomato expression under a fluorescent wide-field microscope (Nikon, Switzerland).

Mouse brain *in vivo* virus stamping. Mice were anesthetized and a 3-mm-diameter cranial window was made above visual cortex. The dura was removed and the cortical surface was kept moist with a solution containing: 125 mM NaCl, 5 mM KCl, 10 mM glucose, 10 mM HEPES, 2 mM $MgSO_4$ and 2 mM $CaCl_2$. The shadow-imaging technique[6,35], with 3–5 MΩ pipettes filled with a solution containing 50 µM Alexa 594, was used to visualize neuronal cells *in vivo*. Pipettes were back-filled with virus-bound magnetic nanoparticles encoding *GFP*. After targeting a single cell using the shadow-imaging approach (with a pipette 45° angle relative to horizontal, using an Olympus BX61WI microscope attached to a MaiTai HP two-photon laser), the pipette tip was brought adjacent to the cell body. Nanoparticles were then pulled down toward the cell body by applying a ~100 mTesla field strength for 3–5 min using an electromagnet (GT-150, Isliker Magnete, Switzerland) positioned at the same angle as the patch pipette (**Fig. 3c**). The magnet was then turned off, the pipette retracted and the cortex was covered with a 3-mm coverslip.

***In vivo* two-photon calcium imaging.** Mice were anesthetized and cells were infected in cortex *in vivo* as described above, except that pipettes were backfilled with magnet nanoparticles bound with either G-deleted rabies viruses encoding *GCaMP6s* or AAVs encoding *GCaMP6s*. Six days after stamping (for rabies) and 18 d after stamping (for AAVs), mice were lightly anesthetized and their heads fixed under a two-photon microscope. Mice were presented with visual stimuli and functional responses were recorded from GCaMP6s-expressing neurons as previously described[6]. The visual stimulus used for these experiments was drifting gratings (i.e., black and white bars) moving in eight directions. For some experiments, the PHP.B serotype of AAV was used to infect neurons and drive widespread expression of GCaMP6s. For these animals, the AAV was injected intravenously via retro-orbital injection, as previously described[38].

Brain organoid production and stamping. Brain organoids were produced as previously described[52]. For shielded stamping experiments, organoids were transferred from an incubator and placed under a two-photon microscope. Shielded stamping was then performed as described above for *in vivo* cortical experiments.

Statistical analysis. Most of the statistical analysis was performed using Prism (version 6.0b for Mac OSX; GraphPad Software) where Mann-Whitney *U*-test was used for all comparisons. The exception was for Pearson correlation coefficients and coefficients of determination, which were performed in Matlab (version 2015b, Mathworks, Nattick, MA). *P* values were not considered significant when $P > 0.05$ (n.s.) and significant when $P < 0.05$ (*) and $P < 0.01$ (**).

Modeling the electromagnet used for virus stamping and its interaction with the virus-coated nanoparticles. To better understand how nanoparticles are manipulated by the magnetic field, we theoretically described the apparatus used for shielded virus stamping experiments. This included a numerical model of the electromagnet, calculations of the forces exerted on the magnetic nanoparticles, and calculations of the nanoparticle velocities (**Supplementary Note 1**).

Life Sciences Reporting Summary. Further information on experimental design is available in the Life Sciences Reporting Summary.

Data availability statement. The data that support the findings of this study are available from the corresponding authors upon reasonable request.

43. Wickersham, I.R., Finke, S., Conzelmann, K.-K. & Callaway, E.M. Retrograde neuronal tracing with a deletion-mutant rabies virus. *Nat. Methods* **4**, 47–49 (2007).
44. Wickersham, I.R., Sullivan, H.A. & Seung, H.S. Production of glycoprotein-deleted rabies viruses for monosynaptic tracing and high-level gene expression in neurons. *Nat. Protoc.* **5**, 595–606 (2010).
45. Gomme, E.A., Faul, E.J., Flomenberg, P., McGettigan, J.P. & Schnell, M.J. Characterization of a single-cycle rabies virus-based vaccine vector. *J. Virol.* **84**, 2820–2831 (2010).
46. Yonehara, K. *et al.* The first stage of cardinal direction selectivity is localized to the dendrites of retinal ganglion cells. *Neuron* **79**, 1078–1085 (2013).
47. Madisen, L. *et al.* A robust and high-throughput Cre reporting and characterization system for the whole mouse brain. *Nat. Neurosci.* **13**, 133–140 (2010).
48. Müller, J., Bakkum, D.J. & Hierlemann, A. Sub-millisecond closed-loop feedback stimulation between arbitrary sets of individual neurons. *Front. Neural Circuits* **6**, 121 (2013).
49. Martinez-Martin, D. *et al.* Resolving structure and mechanical properties at the nanoscale of viruses with frequency modulation atomic force microscopy. *PLoS One* **7**, e30204 (2012).
50. Farrow, K. *et al.* Ambient illumination toggles a neuronal circuit switch in the retina and visual perception at cone threshold. *Neuron* **78**, 325–338 (2013).
51. Gogolla, N., Galimberti, I., DePaola, V. & Caroni, P. Preparation of organotypic hippocampal slice cultures for long-term live imaging. *Nat. Protoc.* **1**, 1165–1171 (2006).
52. Lancaster, M.A. & Knoblich, J.A. Generation of cerebral organoids from human pluripotent stem cells. *Nat. Protoc.* **9**, 2329–2340 (2014).

nature research

Corresponding author(s): Daniel J. Müller and Botond Roska

☐ Initial submission ☐ Revised version ☒ Final submission

Life Sciences Reporting Summary

Nature Research wishes to improve the reproducibility of the work that we publish. This form is intended for publication with all accepted life science papers and provides structure for consistency and transparency in reporting. Every life science submission will use this form; some list items might not apply to an individual manuscript, but all fields must be completed for clarity.

For further information on the points included in this form, see Reporting Life Sciences Research. For further information on Nature Research policies, including our data availability policy, see Authors & Referees and the Editorial Policy Checklist.

Experimental design

1. Sample size

Describe how sample size was determined.

We did not perform hypothesis based experiments therefore we did not have a pre-determined sample size.

2. Data exclusions

Describe any data exclusions.

None

3. Replication

Describe whether the experimental findings were reliably reproduced.

Again, this paper does not really test scientific hypotheses per se, as it is primarily a techniques paper. However, please see text for details on reproducibility and number of trials when applicable.

4. Randomization

Describe how samples/organisms/participants were allocated into experimental groups.

No animals/samples in this paper were randomized. Which cell lines, samples, animals were used are listed throughout the text, in the in figure legends and in the methods.

5. Blinding

Describe whether the investigators were blinded to group allocation during data collection and/or analysis.

No blinding

Note: all studies involving animals and/or human research participants must disclose whether blinding and randomization were used.

6. Statistical parameters

For all figures and tables that use statistical methods, confirm that the following items are present in relevant figure legends (or in the Methods section if additional space is needed).

n/a	Confirmed	
☐	☒	The exact sample size (*n*) for each experimental group/condition, given as a discrete number and unit of measurement (animals, litters, cultures, etc.)
☐	☒	A description of how samples were collected, noting whether measurements were taken from distinct samples or whether the same sample was measured repeatedly
☐	☒	A statement indicating how many times each experiment was replicated
☐	☒	The statistical test(s) used and whether they are one- or two-sided (note: only common tests should be described solely by name; more complex techniques should be described in the Methods section)
☐	☒	A description of any assumptions or corrections, such as an adjustment for multiple comparisons
☐	☒	The test results (e.g. *P* values) given as exact values whenever possible and with confidence intervals noted
☐	☒	A clear description of statistics including central tendency (e.g. median, mean) and variation (e.g. standard deviation, interquartile range)
☐	☒	Clearly defined error bars

See the web collection on statistics for biologists for further resources and guidance.

Nature Biotechnology: doi:10.1038/nbt.4034

Software

Policy information about availability of computer code

7. Software

Describe the software used to analyze the data in this study.	IMARIS

For manuscripts utilizing custom algorithms or software that are central to the paper but not yet described in the published literature, software must be made available to editors and reviewers upon request. We strongly encourage code deposition in a community repository (e.g. GitHub). *Nature Methods* guidance for providing algorithms and software for publication provides further information on this topic.

Materials and reagents

Policy information about availability of materials

8. Materials availability

Indicate whether there are restrictions on availability of unique materials or if these materials are only available for distribution by a for-profit company.	None

9. Antibodies

Describe the antibodies used and how they were validated for use in the system under study (i.e. assay and species).	This is listed in the Methods in the section "Immunohistochemistry". Only commercial available, previously validated antibodies were used. Product numbers are provided for all antibodies.

10. Eukaryotic cell lines

a. State the source of each eukaryotic cell line used.	Hela Kyoto (Gibco-Life technologies, NY, USA), HEK 293T (HEK EcR-293; Invitrogen), BHK-21 cells (ATCC, CCL-10), BSR-VSV-RVG(provided by Matthias Schnell lab) and BHK- B7GG (provided by Edward M. Callaway)
b. Describe the method of cell line authentication used.	None.
c. Report whether the cell lines were tested for mycoplasma contamination.	See Methods section.
d. If any of the cell lines used are listed in the database of commonly misidentified cell lines maintained by ICLAC, provide a scientific rationale for their use.	None.

Animals and human research participants

Policy information about studies involving animals; when reporting animal research, follow the ARRIVE guidelines

11. Description of research animals

Provide details on animals and/or animal-derived materials used in the study.	This is listed in the Methods in the section "Animals"

Policy information about studies involving human research participants

12. Description of human research participants

Describe the covariate-relevant population characteristics of the human research participants.	No humans used

Nature Biotechnology: doi:10.1038/nbt.4034

nature research

Corresponding author(s): Daniel J. Müller and Botond Roska

☐ Initial submission ☐ Revised version ☒ Final submission

Flow Cytometry Reporting Summary

Form fields will expand as needed. Please do not leave fields blank.

Data presentation

For all flow cytometry data, confirm that:

☒ 1. The axis labels state the marker and fluorochrome used (e.g. CD4-FITC).

☒ 2. The axis scales are clearly visible. Include numbers along axes only for bottom left plot of group (a 'group' is an analysis of identical markers).

☒ 3. All plots are contour plots with outliers or pseudocolor plots.

☒ 4. A numerical value for number of cells or percentage (with statistics) is provided.

Methodological details

5. Describe the sample preparation.	See Supplementary Information
6. Identify the instrument used for data collection.	BD Influx
7. Describe the software used to collect and analyze the flow cytometry data.	*BD FACS Sortware*
8. Describe the abundance of the relevant cell populations within post-sort fractions.	Following gating to select for single nanoparticles, fluorescence intensities of at least 15,000 nanoparticles were recorded, the brightest of these nanoparticles were selected and single nanoparticles were dropped into each well of a 96 well plate.
9. Describe the gating strategy used.	The Alexa dye was excited with a 200mW 488 nm laser and emitted light was filtered with a 530/30 band-pass filter and 505 long-pass mirror.

Tick this box to confirm that a figure exemplifying the gating strategy is provided in the Supplementary Information. ☒

Nature Biotechnology: doi:10.1038/nbt.4034